TU Delft

Delft University of Technology

Monopiles subjected to uni- and multi-lateral cyclic loading

S, Nanda; I, Arthur; S, Sivakumar; Donohue, Shane; Gavin, Ken; Mackinnon, P.; Rankin, Barry; Glynn, DG

DOI
10.1680/jgeen.16.00110

Publication date
2017

Document Version
Final published version

Published in
Proceedings of the Institution of Civil Engineers - Geotechnical Engineering

Citation (APA)
S, N., I, A., S, S., Donohue, S., Gavin, K., Mackinnon, P., Rankin, B., & Glynn, DG. (2017). Monopiles subjected to uni- and multi-lateral cyclic loading. *Proceedings of the Institution of Civil Engineers - Geotechnical Engineering*, *170*(3), 246-258. Article 1600110. https://doi.org/10.1680/jgeen.16.00110

Important note
To cite this publication, please use the final published version (if applicable).
Please check the document version above.

Copyright
Other than for strictly personal use, it is not permitted to download, forward or distribute the text or part of it, without the consent of the author(s) and/or copyright holder(s), unless the work is under an open content license such as Creative Commons.

Takedown policy
Please contact us and provide details if you believe this document breaches copyrights.
We will remove access to the work immediately and investigate your claim.

This work is downloaded from Delft University of Technology.
For technical reasons the number of authors shown on this cover page is limited to a maximum of 10.

Geotechnical Engineering

Monopiles subjected to uni- and multi-lateral cyclic loading
Nanda, Arthur, Sivakumar *et al*.

ice | proceedings

Proceedings of the Institution of Civil Engineers

http://dx.doi.org/10.1680/jgeen.16.00110
Paper 1600110
Received 30/06/2016 Accepted 29/11/2016
Keywords: models (physical)/offshore engineering/piles & piling

ICE Publishing: All rights reserved

ice Institution of Civil Engineers
publishing

Monopiles subjected to uni- and multi-lateral cyclic loading

1 **Satyajeet Nanda** BTech, MTech, PhD
Postdoctoral Research Fellow, School of Natural and Built Environment, Queen's University Belfast, Belfast, UK

2 **Iain Arthur** MEng
PhD Student, School of Natural and Built Environment, Queen's University Belfast, Belfast, UK

3 **Vinayagamoorthy Sivakumar** BSc, MSc, DIC, PhD, DSc, CEng, PGCHET, FICE
Reader, School of Natural and Built Environment, Queen's University Belfast, Belfast, UK (corresponding author: v.sivakumar@qub.ac.uk)

4 **Shane Donohue** BSc, PhD, FHEA
Lecturer, School of Natural and Built Environment, Queen's University Belfast, Belfast, UK

5 **Aaron Bradshaw** PhD, PE
Assistant Professor, University of Rhode Island, Department of Civil and Environmental Engineering, Kingston, RI, USA

6 **Ryan Keltai** MEng
Graduate Engineer, McAdam Design, Belfast, UK

7 **Ken Gavin** BEng, PhD, CEng
Professor of Subsurface Engineering, Geo Engineering, Faculty of Civil Engineering and Geosciences, TU Delft, CN Delft, the Netherlands

8 **Pauline Mackinnon** BEng, PhD, MICE, CEng
Senior Lecturer, School of Natural and Built Environment, Queen's University Belfast, Belfast, UK

9 **Barry Rankin** BSc, PhD, CEng, MICE
Construction Division Manager and Honorary Senior Lecturer, Queen's University Belfast, Belfast, UK

10 **Danny Glynn** BSc, Cert Law, CEng, CEnv, FICE
Director, Byrnelooby, Belfast, UK










Offshore wind turbines are subjected to significant environmental loads from a combination of current, wind and wave action. Under such conditions, the directions of these environmental loads vary over the service life of the structure and therefore the cyclic lateral loading on the foundation also changes direction. The work reported in this paper examines the effects of multi-directional loading on the performance of offshore wind turbine monopile foundations. Tests were carried out in a model sand bed and a mobile loading platform was manufactured to apply loading on the pile in various directions. Tests were also carried out where the cyclic loading was applied under both one-way and two-way loading. The observations indicate significant differences in the stiffness of monopiles between uni-directional and multi-directional lateral cyclic loading. Multi-directional lateral cyclic loading generally results in higher displacements and lower stiffness compared to uni-directional loading, most likely due to shear deformation of a larger volume of soil mass adjacent to the pile.

Notation

A_H	dimensionless constant
A_N	dimensionless model parameter
C_1	constant
D	pile diameter
F_s	mobilised skin friction
G	soil modulus
H	horizontal load
H_{max}	maximum horizontal loads in a cycle
H_{min}	minimum horizontal loads in a cycle
$\tilde{H}$	dimensionless horizontal load
K_P	coefficient of passive earth pressure
$\tilde{k}$	dimensionless stiffness
k_0	dimensionless stiffness at $N = 1$
L	embedment depth of monopile
m	applied moment on monopile
N	number of cycles
P_R	reference stress
r'	model parameter
t	model parameter
u	radial displacement
u_0	radial displacement at $N = 1$
$\tilde{u}$	dimensionless horizontal displacement
W	total weight of pile

Downloaded by [TU Delft Library] on [08/02/17]. Copyright © ICE Publishing, all rights reserved.

Z	observed vertical displacement
$\tilde{Z}$	dimensionless vertical displacement
α	total angle to be covered during multi-directional loading
β	angle between loading direction and x-axis
γ'	soil density
$\Delta\theta$	rotational displacement of monopile at soil surface
δ	angular interval between two successive loadings
θ	direction of loading from the x-axis at cycle N from the initial ($N = 1$) location of the monopile
ξ	load parameter
σ'_v	effective vertical stress

1. Introduction

Offshore wind turbines are increasingly being used to harness the energy from relatively frequent and powerful winds prevalent in the marine environment. The offshore wind turbine is a complex structure and experiences a combination of static, cyclic and dynamic loads. Monopiles are usually used as the foundation for offshore wind turbines. The resistance of monopiles to cyclic horizontal load is designed based on the recommendations provided by various agencies such as the American Petroleum Institute (API-RP-2A (API, 2000)), and the marine certification authority Det Norske Veritas (DNV, 2011) and so on. These recommendations are primarily based on experience gained from small-diameter piles with a few cycles of uni-directional load and are not necessarily applicable to larger diameter piles (Murchison and O'Neill, 1984; Reese and Van Impe, 2011). Furthermore, this method is limited in that it does not include the number of cycles as a parameter to predict the response to cyclic lateral load (Achmus *et al.*, 2009; Leblanc *et al.*, 2010; Rudolph *et al.*, 2014). Wind turbines also have strict serviceability requirements for permanent rotation. In offshore wind turbines the dynamic/cyclic loadings are mainly coming from environmental (wind and wave) load, along with rotor and blade motions. The common practice adopted for wind turbine design is the 'soft–stiff structure' which requires the natural frequency to be in the range between 1P and 3P, where 1P represents the frequency band for the rotor and 3P is that for the blade motion. Any change in natural frequency may adversely affect the longevity of the wind turbine system. The natural frequency changes with the variation in soil–monopile stiffness. Various studies suggest that this soil–monopile stiffness changes with the number of loading cycles. In addition the studies have also demonstrated that the soil properties change with the dynamic/cyclic loading. Therefore it may be anticipated that soil–monopile stiffness will also change with cyclic loading.

Monopiles consist of open-ended steel pipe piles installed in water depths of about 10 to 30 m. The diameter and length of monopiles depend on various factors including the wind turbine capacity, subsurface conditions, the installation procedure, and the intensity and nature of the environmental loading. The diameter of monopiles currently used in offshore wind turbines ranges from 3 to 7 m and L/D (L = embedment length and D = diameter of pile) ratios are usually less than 12. The L/D ratios of piles used in onshore or offshore oil and gas structures ranges from 20 to 200 with diameters in the range of 0·5 to 3 m. A typical ratio between the horizontal and vertical loads for piles used in oil and gas structures is 0·25, whereas for wind turbines it may vary from 0·6 to 2·6 (Houlsby *et al.*, 2005; Schneider and Senders, 2010). As the soil–pile interaction and load transfer mechanisms are distinctly different for monopiles used for offshore wind turbines and piles used for oil and gas structures, the parameters used in the design of such structures should also be different. As monopiles are short, they resist horizontal cyclic load by developing passive resistance along their entire length. This makes the monopiles 'free headed' (i.e. almost unrestricted in the movement of the pile) and more vulnerable to tilt (Cui and Bhattacharya, 2016), whereas the piles used for oil and gas structures develop significant restraint at the pile head owing to high embedment depth.

The main issue with a monopile subjected to horizontal cyclic loading is to predict how much horizontal displacement (or rotation) will occur at given amplitude of cyclic load. Numerous studies have been reported on the behaviour of piles under horizontal cyclic loading (Alizadeh and Davisson, 1970; Bienen *et al.*, 2012; Dyson and Randolph, 2001; Little and Briaud, 1988; Reese and Van Impe, 2011; Tucker and Briaud, 1988). However, the majority of these studies were developed for flexible piles for offshore oil and gas platforms. Offshore structures are subjected to significant environmental loads from a combination of waves, current and wind action. These environmental loads induce high numbers of cycles (about 10^7 to 10^9) of lateral loading on the foundations over the life span of the structure. A number of studies have investigated monopile behaviour under large numbers of cycles and uni-directional loading (Arshad and O'Kelly, 2016; Chen *et al.*, 2015; Leblanc *et al.*, 2010; Li *et al.*, 2010, 2015; Murphy *et al.*, 2016; Peng *et al.*, 2011). These studies were conducted at small L/D ratios and various mechanisms such as winged monopiles (Murphy *et al.*, 2016) and piled cruciform (Arshad and O'Kelly, 2016) were examined to reduce the horizontal moment. The loading direction in these studies remained constant. Under offshore conditions, the direction of the environmental load changes with time over the life of the structure and therefore so does the direction of the horizontal cyclic loads acting on the monopile. The angle between the direction of the wind and waves is not always co-linear, and may vary by as much as 90° (Seidel, 2010). Rudolph *et al.* (2014) investigated the effects of multi-directional cyclic loading on monopiles and found significant differences in the results when compared to uni-directional cyclic loading. Although Rudolph *et al.* (2014) used a loading pattern close to the actual loading pattern for an offshore monopile, the piles were tested under one-way cyclic loading.

Downloaded by [TU Delft Library] on [08/02/17]. Copyright © ICE Publishing, all rights reserved.

The aim of the research reported in this paper is to investigate the response of monopiles subjected to multi-directional loading (one-way and two-way) and to compare this with the response of piles subjected to uni-directional loading. A number of uni-directional and multi-directional cyclic lateral load tests were carried out on closed-ended as well as open-ended piles under two cyclic load patterns. The results are presented in dimensionless form. The response of closed-ended piles was investigated as part of the research as there are reasons to suggest that open-ended piles could become closed-ended due to soil plugging in the long term. An additional reason includes the use of precast concrete monopiles (closed-ended) as a measure to reduce the cost of construction.

2. Experimental programme

The monopile used in the experiments was manufactured using a steel pipe with an external diameter of 90 mm and a wall thickness of 5 mm. The length of the pile was restricted to 900 mm (including a 370 mm length of pile protruding above the soil layer), resulting in an L/D ratio of 10. In comparison to a typical monopile of 4 m diameter, the scale of this model monopile is about 1/40. More on scaling law will be discussed in Section 4 on dimensionless equations. The close-ended configuration was achieved by welding a steel plate on one end of the steel pipe. The depth of pile penetration into the soil bed was restricted to 530 mm. Three metal plates were attached to the pile at the point of displacement measurements in the X–Y–Z directions, as shown in Figure 1. Displacement transducers were supported on individual frames attached to the testing chamber.

The soil bed was formed in a rigid chamber (700 cm wide, 700 cm long and 740 cm high). The soil used for testing consisted of dry building sand with D_{10}, D_{30} and D_{60} of 0·2 mm, 0·25 mm and 0·35 mm, respectively. The peak and ultimate angles of internal friction at low stress level of the material were 37° and 34°, respectively. In laboratory model tests, there is always some boundary wall effect on the test results. Bhattacharya *et al*. (2013) found that the soil mass influenced by dynamic loads on suction caisson foundations reduces exponentially with the lateral distance away from the point of loading. The effect becomes insignificant at a distance of 5D (where D is the diameter of the pile) from the centre of the foundation. Since the distance between the rigid chamber wall and the centre of the pile is more than 4D in the present investigation, it would be expected that the test results may not be affected significantly due to the rigid boundary wall.

Two buckets of sand (each 10 l in volume) were poured into the chamber in stages and the surface was levelled. At each stage, the level of sand in the test chamber was raised by approximately 60 mm and, after each stage, the soil bed was compacted evenly for 2 min using a vibrating plate, which achieved a target density of approximately 1700 kg/m^3. The average relative density achieved during this investigation was about 77%. The pile base was supported on a sand bed 90 mm thick. The pile was then located centrally in the testing chamber and further sand was added, adopting the same procedure in order to build up the sand bed to a height of 620 mm. In the case of the open-ended pile, the bottom end of the pile was temporarily blocked and sand was compacted into the pile to the same height as that of the testing bed. The pile was then gently moved inside the testing bed and located in place. The temporary blockage at the end of the pile was carefully removed.

In order to apply multi-directional cyclic loads to the pile, a two-way loading chamber was mounted on a mobile platform. A circular metal hook was then attached to the end of the loading actuator, as shown in Figure 1. During testing, the hook was placed around the circular pile. The inner diameter of the hook was 5 mm larger than the outer diameter of the pile in order to account for any pile misalignment that could occur after cycles of repeated loading. The inner surface of the hook was curved so that the interaction between the pile and the loading hook was smooth with reduced friction. The rear end of the actuator was pressurised to a constant pressure and the pressure in the front of the chamber (where the loading ram protrudes) was controlled using an automated pressure controller (APC). A gearbox was utilised to rotate the actuator in the desired direction (Figure 1). The gearbox has a manual setting to change the rotational speed of the drive shaft. One end of a channel bracket was attached to the drive shaft on the gearbox. The loading chamber was attached to the other end of this bracket. It was mounted in such a way that it could rotate around the pile vertical axis to take account of any misalignment of the pile. A control program (supplied by VJ Tech Limited, UK) facilitated the application of cyclic loading using a triangular wave form.

3. Applied load pattern and loading direction

One-way and two-way triangular waveforms were applied depending on the test requirements of the present research. In most of the tests, 1000 or more cycles were applied with a uniform loading amplitude of 540 N (Table 1). In one of the tests, however, due to excessive vertical displacement of the pile it was only possible to carry out 350 cycles. The loading frequency in offshore conditions can vary during the lifetime of a pile and is typically in the range of 0·05–0·2 Hz (Lesny and Hinz, 2009). Since the main objective of this research was to find monopiles' response under changing load direction, the loading frequency remained constant throughout the investigation. The loading frequency of 0·02 Hz was used in all tests. The monopile response to the change in loading frequency in the range of 0·02–0·2 Hz may not influence much, as dry cohesionless soil does not show much change in properties with change in shearing strain rate (discussed in Sathialingam and Kutter (1989)).

Downloaded by [TU Delft Library] on [08/02/17]. Copyright © ICE Publishing, all rights reserved.

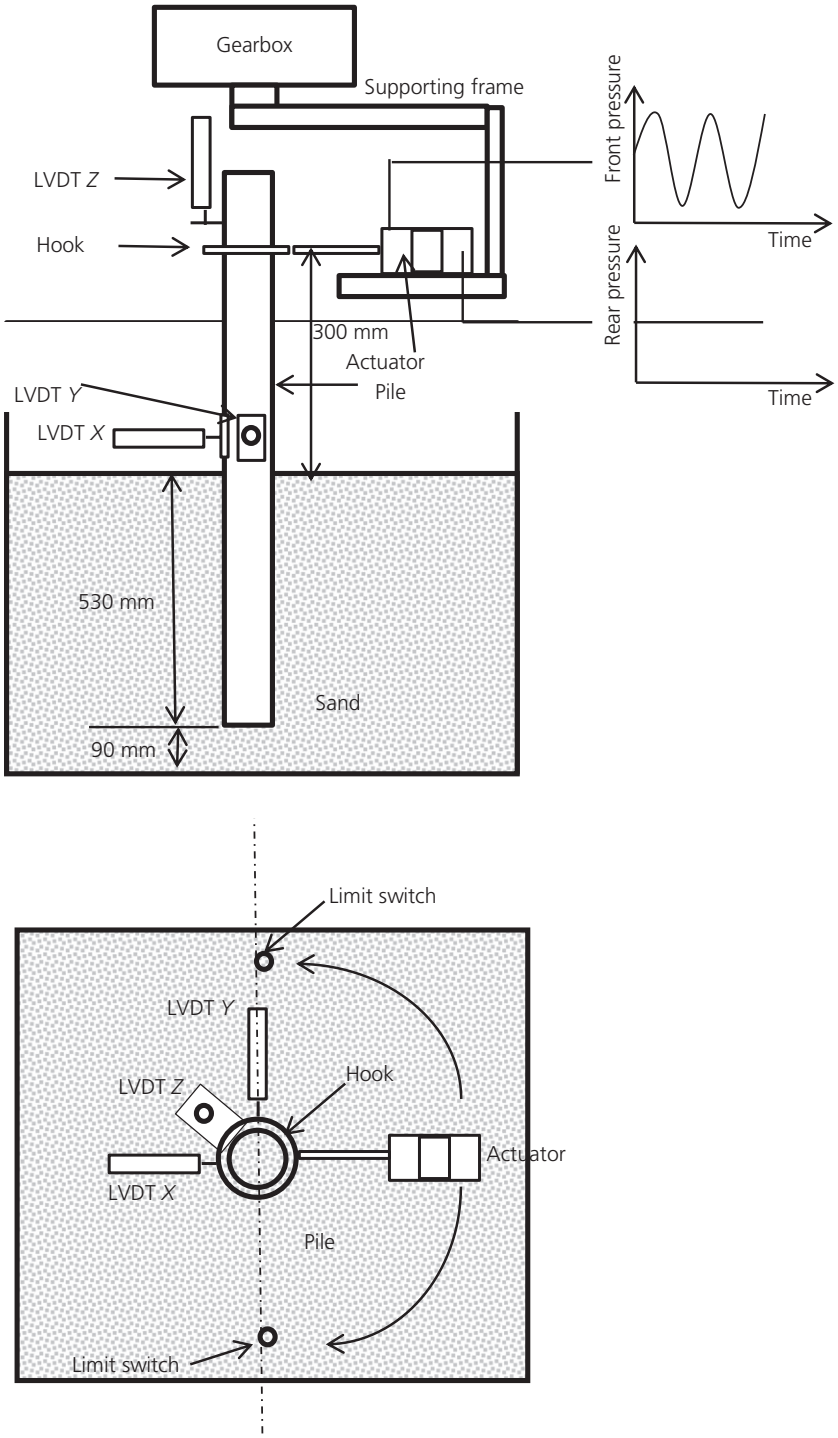

Figure 1. Testing configuration

In total, eight model tests were carried out, among which seven were cyclic tests and one was a monotonic test. Table 1 provides details of all cyclic tests carried out. In four of the tests, the pile was subjected to multi-lateral loading. In order to achieve this, two limit switches were located on a cross-beam, overhanging the testing bed, as shown in Figure 1. In tests 4 and 5, the loading pattern was one-way and in tests 6 and 7 the loading pattern was two-way with multi-directional loading.

For cyclic loading, the load amplitude remained uniform through the investigation, but the cyclic load pattern and load

Downloaded by [TU Delft Library] on [08/02/17]. Copyright © ICE Publishing, all rights reserved.

Table 1. List of tests

Test no.	Pile end type	Loading direction	H_{max}: N	H_{min}: N	ξ	α	δ	u_0: mm	k_0	A_H	A_N	t
T_0	C	Monotonic load test	—	—	—	—	—	—	—	—	—	—
T_1	O	U	540	0	0	0	0	1·53	2535	650	0·5	0·18
T_2	O	U	540	−540	−1	0	0	2·69	2117	400	—	—
T_3	C	U	540	−540	−1	0	0	2·64	2525	100	—	—
T_4	O	M	540	0	0	180	4·5	1·84	2357	1000	0·5	0·5
T_5	C	M	540	0	0	180	4·5	2·52	2659	1300	0·5	0·4
T_6	O	M	540	−540	−1	180	4·5	2·85	2140	−100	—	—
T_7	C	M	540	−540	−1	180	4·5	2·62	—	—	—	—

C, closed ended; O, open ended; U, uni-directional; M, multi-directional; H_{min}, minimum horizontal loads in a cycle; H_{max}, maximum horizontal loads in a cycle; ξ, load parameter; $\bar{k}_0$, dimensionless stiffness at $N = 1$

direction were changed considerably between experiments. In order to characterise the applied cyclic load, a load parameter was used, which can be defined as

$$\xi = \frac{H_{min}}{H_{max}} \quad (1)$$

where H_{min} and H_{max} are the minimum and maximum horizontal loads in a cycle. The value of ξ can vary between 1 and −1. $\xi = 1$ represents non-cyclic loading, whereas $\xi = 0$ and $\xi = -1$ represent one-way and two-way cyclic loading, respectively. In general, the ξ value varies in the range −0·5–1 under offshore loading conditions. However, in order to study the extreme limits of the cyclic loading effect, ξ in the range from 1 to −1 was used in the present investigation (Table 1).

The direction of environmental loading (wind, waves and so on) changes over the lifespan of an offshore structure. A simple experiment was designed to study the effect of multi-directional cyclic loading on monopile response. In this investigation multi-directional load was applied by changing the direction of the load for every loading cycle. The multi-directional load used in this investigation is depicted in Figure 2(a). For example, multi-directional loads move at an interval of $\delta = 4{\cdot}5^{\circ}$ and are applied in a region comprising $\alpha = 150^{\circ}$. In Figure 2(a), the first horizontal cyclic load ($N = 1$) starts along the x-axis and thereafter moves towards to the limit switch A_1 with an interval of 4·5° between each cycle. At $N = 16$ it touched the limit switch A_1 and thereafter moved towards the limit switch B_1 at $N = 46$. The multi-directional loading depicted in Figure 2(a) can be expressed mathematically in terms of the loading direction from the initial location of the monopile at a given load cycle number (N) as

$$\theta = \frac{\alpha}{180} \sin\left[\sin^{-1}\frac{180\delta(N-1)}{\alpha}\right] \quad (2)$$

where θ is the direction of loading from the x-axis at cycle N from the initial ($N = 1$) location of the monopile; N is the number of cycles; α is the total angle to be covered during multi-directional loading; and δ is the angular interval between

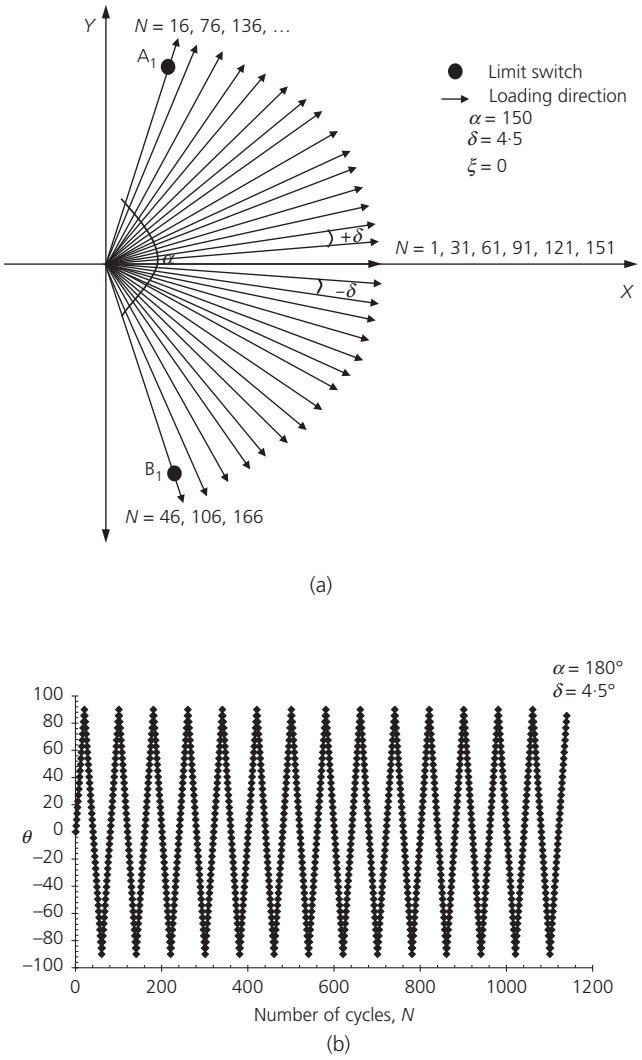

Figure 2. (a) Multi-directional loading direction. (b) The θ–N used in this investigation

two successive loadings. Figure 2(b) shows the value of N and the corresponding value of θ used in this investigation. The values of α and δ used in model tests were 150° and 4·5°,

Downloaded by [TU Delft Library] on [08/02/17]. Copyright © ICE Publishing, all rights reserved.

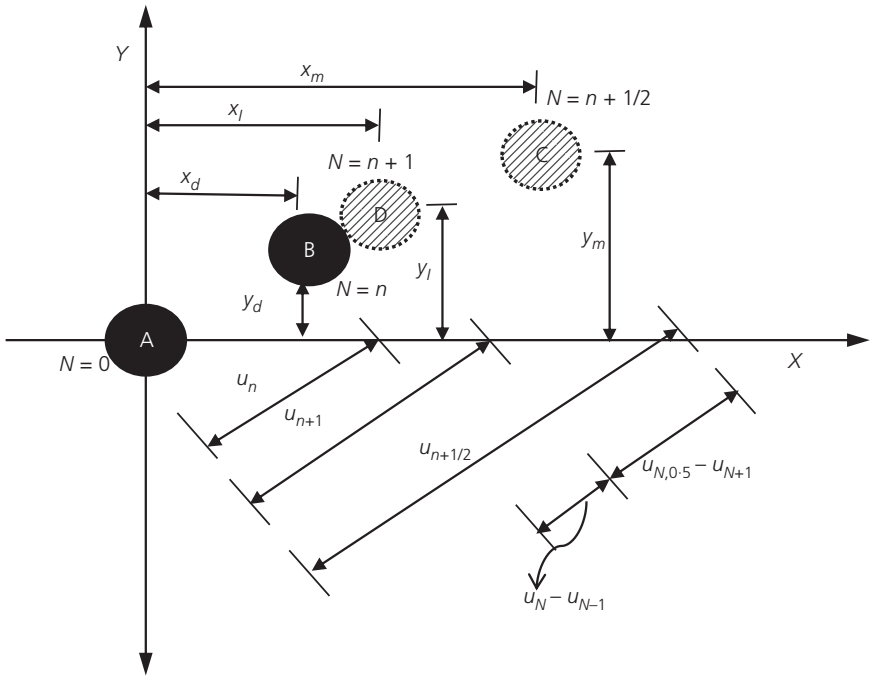

Figure 3. Location of pile from origin

respectively. Equation 2 can also be utilised to calculate the location of the pile at a given load cycle N. At a given load cycle number N the location of pile will be

3. $$x_I = x_d + (u_{n+1} - u_n)\cos\beta$$

4. $$y_I = x_d + (u_{n+1} - u_n)\sin\beta$$

where x_I, y_I, x_d, y_d and u_n are defined in Figure 3. β is the angle between the line joining points B, D and the x-axis, which is the same as θ, if the loading path is a straight line in the x–y plane. Table 1 shows details of the multi-directional loading used in the present investigation.

4. Dimensionless equations

The present investigation on monopiles is based on laboratory experiments on small-scale models. To enhance its applicability at full scale, scaling effects may be considered by expressing the results in dimensionless form. Leblanc *et al.* (2010) proposed that, for a monopile, the elastic response in terms of applied moment and displacement angle can be expressed as

5. $$m = \left[\frac{GL^2D(k_1k_3 - k_2^2)}{k_3 - k_2(HL/m)}\right]\Delta\theta$$

where m is the applied moment on the monopile; $\Delta\theta$ is the rotational displacement of the monopile at the soil surface; k_1, k_2, k_3 are dimensionless constants; G denotes the soil modulus; D is pile diameter; H is horizontal load; and L is the embedment depth of the monopile. The majority of published studies on the lateral load response of piles are presented in terms of the horizontal load–displacement relationship. API (2000) also uses the p–y relationship (where, p is lateral resistance and y is lateral displacement) to design the lateral load response of monopiles. Equation 5 can be rearranged in terms of horizontal load and displacement to give

6. $$H = \left\{\frac{GD(k_2^2 - k_1k_3)}{[k_2(m/HL) - k_1]}\right\}u$$

The value of G for soil is a stress-dependent property and various studies suggest that it can be expressed as a function of stress as

7. $$\frac{G}{P_R} = k_1\left(\frac{\sigma'_v}{P_R}\right)^r$$

where P_R is the reference stress; σ'_v is the effective vertical stress; and r is a model parameter. Leblanc *et al.* (2010) suggested that the vertical effective stress along the pile depth can be expressed as

8. $$\sigma'_v = C_1L\gamma'$$

where γ' is the soil density and C_1 is a constant. Substituting Equations 7 and 8 into Equation 6 and expressing in

Downloaded by [TU Delft Library] on [08/02/17]. Copyright © ICE Publishing, all rights reserved.

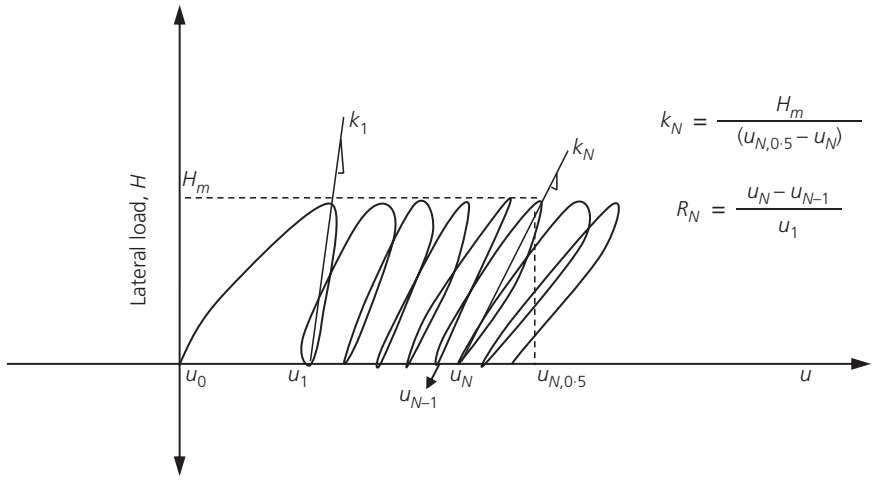

Figure 4. Definition of various parameters

non-dimensional form results in the following equation

$$9. \quad \frac{H}{DL^2\gamma'} = \frac{k_1\sqrt{C_1}\left(k_3^2 - k_3k_1\right)}{k_2(m/HL) - k_1}\sqrt{\frac{P_R}{L\gamma'}}\left(\frac{u}{L}\right)$$

Equation 9 can be rewritten as

$$10. \quad \tilde{H} = \tilde{k}\tilde{u}$$

where

$$\tilde{H} = \frac{H}{DL^2\gamma'}; \quad \tilde{k} = \frac{k_1\sqrt{C_1}\left(k_3^2 - k_3k_1\right)}{k_2(m/HL) - k_1}; \quad \tilde{u} = \sqrt{\frac{P_R}{L\gamma'}}\left(\frac{u}{L}\right)$$

In the above equation $\tilde{H}$, $\tilde{k}$ and $\tilde{u}$ represent dimensionless quantities for horizontal load, stiffness and horizontal displacement, respectively.

5. Results and discussion

The results of the model tests are presented in dimensionless form, expressed as a function of the number of cycles. Emphasis has been given to the change in stiffness of the soil–pile system and its displacement response. For data analysis, the initial position of pile ($N = 0$) is considered as the origin and any change in subsequent load cycles was measured with respect to the origin. In Figure 3, point A is the location of the pile before application of any cyclic load ($N = 0$) and point B is the location of the pile after n cycles of loading ($N = n$). The displacement of the pile after $N = n$ is u_n, which can be calculated as

$$11. \quad u_N = \sqrt{x_d^2 + y_d^2}$$

Point C represents the location of the pile after application of the maximum horizontal load from point B ($N = n + 1/2$) and point D represents the pile location after $N + 1$ cycles. The method and definition of parameters used for data analysis are given in Figure 4. The soil–pile response to the horizontal cyclic load is expressed in three different parameters by evaluating stiffness and accumulated deformation. These parameters are defined in Equations 12 and 13.

$$12. \quad k_N = \frac{H_m}{\left(u_{N,\,0·5} - u_{N+1}\right)}$$

$$13. \quad R_N = \frac{u_N - u_{N-1}}{u_1}$$

All these parameters are expressed and discussed as a function of the number of cycles (N). k_N represents the initial stiffness of the soil–pile response. R_N describes the permanent displacement in u_N–H space between two successive load cycles. The dimensionless equation for the above parameter may be derived from Equation 10 as

$$14. \quad k_N = \frac{k_N}{D\sqrt{\gamma' L P_R}}$$

5.1 Monotonic load test

The amplitude for cyclic loading was determined from the response of the monopile when subjected to monotonic horizontal loading (Figure 5) and the target loading of 540 N corresponds to 0·5° of rotation on the assumption that the rotating point was at the base. During the monotonic load

Downloaded by [TU Delft Library] on [08/02/17]. Copyright © ICE Publishing, all rights reserved.

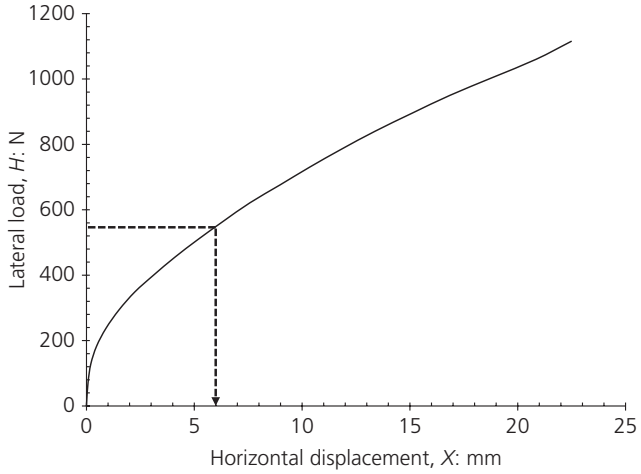

Figure 5. Control test, monotonic loading (T_0)

test, the loading on the pile was applied in steps of 50 N and each time the loading was maintained for 5 min.

5.1.1 Cyclic load test

Figure 6(a) shows a typical response of the open-ended pile subjected to uni-directional loading with 1600 loading cycles (T_1). The loading was applied in the X direction and the displacement of the pile in the X, Y (horizontal) and Z (vertical) directions was continuously monitored. The displacement of the pile in the Y direction is not reported, as no loading was applied in that direction. The displacement along the X direction on the first application of the loading was about 2·8 mm, which is considerably smaller than that observed from monotonic loading conditions (Figure 5) at the same magnitude of loading. Under monotonic loading conditions, the load was applied in stages and was maintained for 5 min. It was observed during this staged loading, that the displacement of the pile was time dependent, although one would expect it to be instantaneous as the soil bed was made of dry sand. The time-dependent behaviour in this case is likely to have been caused by gradual loosening of the sand close to the active side of the pile and consequently the sand on the passive side gradually moving into the active side during the resting period. However, in the case of cyclic loading, the rate of loading was fast without any resting period.

The response of the closed-ended piles for selected loading cycles under uni-directional two-way loading is highlighted in Figure 6(b). Interestingly, the pile continued to move laterally throughout the test, even after large numbers of cycles. Note that the terms 'closed-ended' and 'open-ended' refer to the pile's end condition before installation. In the case of the open-ended pile with similar loading conditions (and similar number of cycles) the lateral displacement was about 2 mm (after 1000 loading cycles, Figure 6(c)) and when the end condition of the pile was closed, the lateral displacement was about 5 mm (after 1075 loading cycles, Figure 6(b)). Figure 6(d) shows the displacement along the X- and Y-axes with the number of cycles in multi-directional loading for test T_6. It appears that the displacement progressively increased in the X direction until up to approximately 200 loading cycles and then a steady state was gradually achieved (note that the data between the 230th and 390th cycles were not recorded owing to a fault in the data logger). Similar observations were made along the Y direction, although the magnitude of displacement is somewhat lower than that observed in the X direction. Figures 6(a)–6(d) show some of the raw data recorded during the model test. In subsequent sections the recorded data will be further analysed and presented in terms of design parameters such as stiffness, lateral and vertical pile settlement. Figure 6(e) shows the lateral load and u_N relationship (as discussed in Equation 11 and Figure 4) for test T_4 at selective loading cycles.

5.2 Stiffness

The dimensionless stiffness of the soil–pile system, as shown in Equation 14 and defined in Figure 4, was considered for stiffness analysis. Figures 7(a)–7(c) show the variation of soil–pile stiffness as a function of N under horizontal cyclic loading (uni-directional (U)/multi-directional (M), one-way ($\xi = 0$) and two-way ($\xi = -1$) loading). Horizontal loading on the monopile produces both passive and active conditions in the adjacent soil mass. With each passing cycle of load, the soil mass produces resistance with some permanent displacement to the soil–pile system. With an increase in the number of cycles of loading, the soil–pile system proceeds towards a final equilibrium condition where changes in soil–pile response are minimal. $\tilde{k}$ is highly scattered but the overall trend shows an increase in the stiffness with N. The high variability in $\tilde{k}$ may be due to the formation as well as breakage of any dense/loose sand conditions, particularly close to the pile, before achieving a stable soil–pile equilibrium condition. Consistent with LeBlanc *et al.* (2010), the change in soil–pile stiffness observed in this investigation can be expressed conveniently using the following logarithmic function

$$k_N = k_0 + A_H \ln(N) \quad (15)$$

where, A_H is a dimensionless constant and k_0 is the dimensionless stiffness at $N = 1$. Values of A_H and k_0 are given in Table 1. The lines shown in Figure 7 were drawn using Equation 15. The maximum variation of k_0 is about 15%. The values of A_H are an indication of stiffness improvement with cyclic loading under various loading conditions. For example, A_H for one-way loading was 650 (T_1), reducing to 400 under two-way loading (T_2). Under multi-directional one-way loading (T_4) the stiffness A_H increases to 1000. Further discussion of this parameter is presented later in this article. Owing to some technical difficulties, only 350 cycles of data were available for T_7.

Downloaded by [TU Delft Library] on [08/02/17]. Copyright © ICE Publishing, all rights reserved.

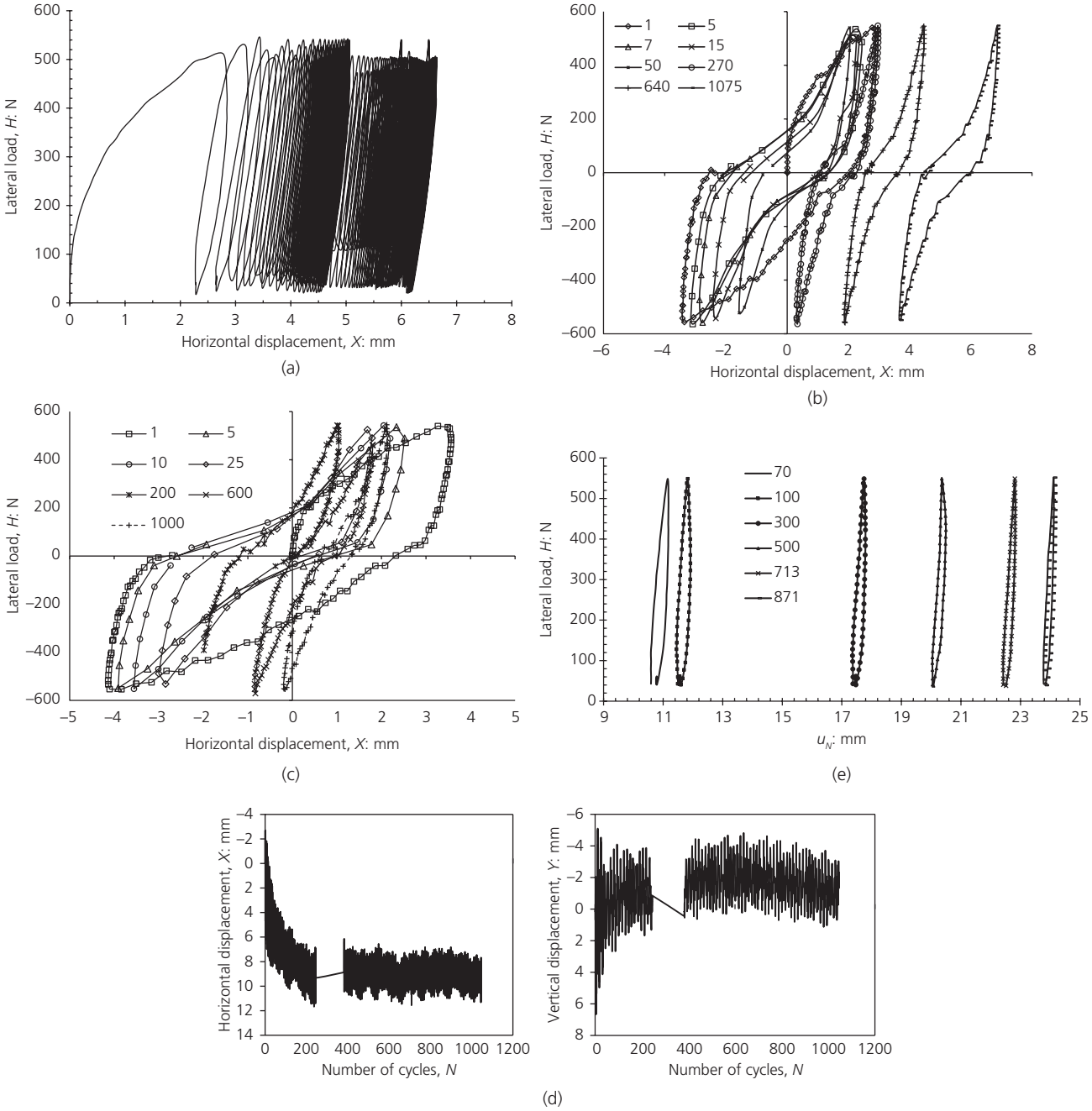

Figure 6. (a) Performance of monopile (open-ended) during lateral loading (T_1, U, O, $\xi = 0$). (b) Horizontal displacement and lateral load relationship at various cycles of loading for uni-directional closed-ended pile (T_3, U, C, $\xi = -1$). (c) Horizontal displacement and lateral load relationship at various cycles of loading for uni-directional open-ended pile (T_2, U, O, $\xi = -1$). (d) Observed pile movement along *X*- and *Y*-axis with number of cycles during multi-directional test (T_6, M, O, $\xi = -1$). (e) Lateral load and u_N relationship at various cycles (T_4, M, O, $\xi = 0$)

5.3 Displacement

The present investigation measured both horizontal displacements (*X*-axis and *Y* axis) and vertical displacement (*Z* axis). In order to present the measured pile location from its initial position, the radial distance as described in Equation 11 has been used to describe the pile displacement. Figure 8 shows the change in radial displacement with the number of cycles. The results are presented in dimensionless form in terms of u_N/u_1, where u was obtained from Equation 11. Two distinct patterns in accumulated displacement may be observed between $\xi = 0$ (Figure 8(a)) and $\xi = -1$ (Figure 8(b)). At $\xi = 0$, displacement continuously increased with each loading cycle

Downloaded by [TU Delft Library] on [08/02/17]. Copyright © ICE Publishing, all rights reserved.

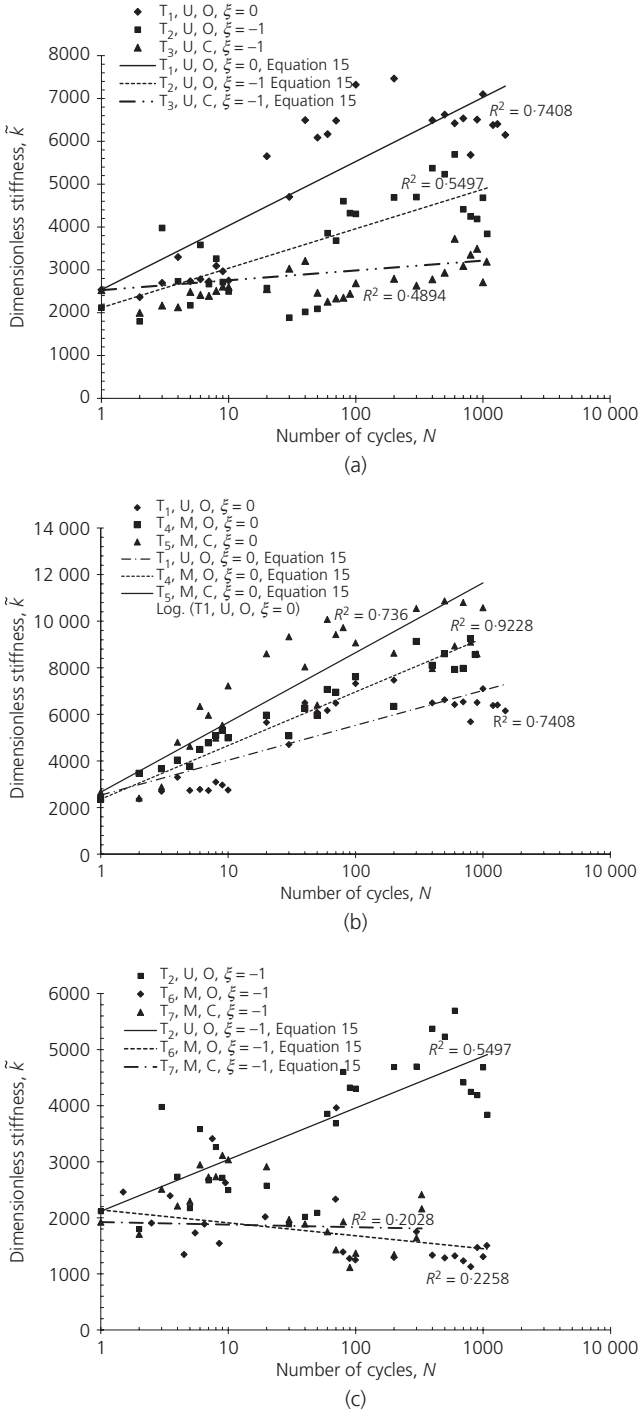

Figure 7. (a) Result of uni-directional loading (open-ended, closed-ended, and one- and two-way loading). (b) Multi-directional loading 180° one-way only (multi-directional, uni-directional and open/closed-ended). (c) Multi-directional loading 180° two-way only (uni-directional and multi-directional, open/closed-ended, two-way loading)

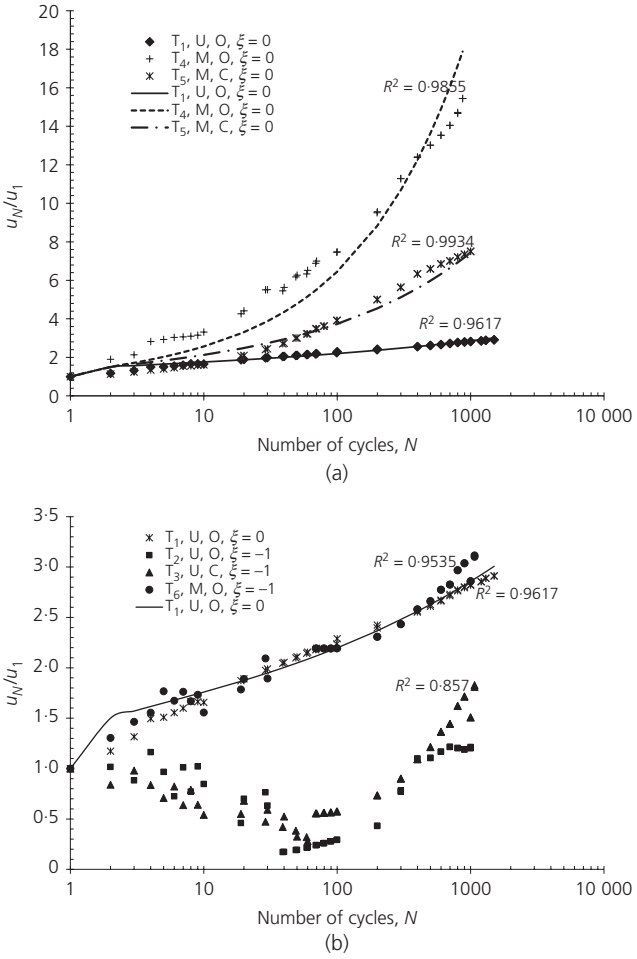

Figure 8. (a) Radial displacement u_N with load cycles for one-way uni-directional and multi-directional loading. (b) Radial displacement u_N with load cycles for two-way uni-directional and multi-directional loading

whereas, for $\xi = -1$, displacement increased for the first few cycles and then reduced with load cycle until N reached about 100 cycles and thereafter it increased again with increasing load cycles. Multi-directional loading produced higher displacements than uni-directional loading. The displacements under $\xi = 0$ cyclic loading can be expressed as a function of N

$$\frac{u_N}{u_1} = 1 + A_N(N-1)^t \quad (16)$$

The value of A_N is 0·5 and values for t are 0·18, 0·5 and 0·4 for tests T_1, T_4 and T_5 respectively (tests conducted with different end conditions either under uni-directional or multi-directional loading). Figure 9 shows the variation in $|R_n|$ with load cycle number ($|R_n|$ is defined in Equation 13). A decrease in $|R_n|$ can be observed with the increase in N value. A decrease in $|R_n|$ signifies a reduction in permanent displacement between two successive cycles and therefore indicates that the soil–pile system is moving towards more elastic behaviour.

Downloaded by [TU Delft Library] on [08/02/17]. Copyright © ICE Publishing, all rights reserved.

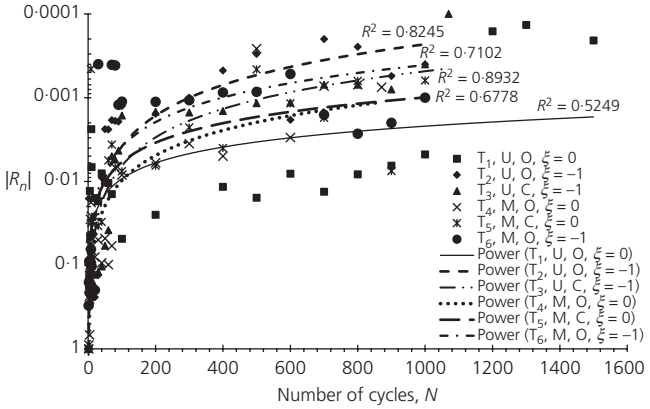

Figure 9. Variation of R_N with N

Looking at the trend lines in Figure 9, a two-way cyclic load ($\xi = -1$) produces a negative value of $|R_n|$.

Figure 10 shows the development of vertical displacements of the monopiles with N. In contrast to long, flexible piles, cyclic loading can induce vertical displacements in monopiles. The vertical displacements can be upward or downward depending upon the direction of soil movement, load amplitude, change in end bearing resistance, weight of monopiles and direction of skin friction. In the case of upward soil movement with higher mobilised skin friction, the vertical component of force along the pile surface will be upward and, when this upward force is more than the total weight on the pile, it produces a vertical upward movement of the pile. In the present investigation vertical upward movement of the pile was observed in all tests. The vertical displacement can be expressed in dimensionless form as

$$17. \quad \tilde{Z} = \frac{\gamma' L F_s K_P D}{W} Z$$

where F_s is the mobilised skin friction; K_P is the coefficient of passive earth pressure; W is the total weight of the pile; and Z is the observed vertical displacement. In Equation 17 the term $\gamma' L F_s K_P D$ represents the component of vertical force along the pile surface. The values of K_P and F_s used in this analysis are 3·3 and 0·8, respectively. Figure 10 indicates that two-way cyclic loading ($\xi = -1$) produces a height $\tilde{Z}$ in comparison with one-way ($\xi = 0$) cyclic loading.

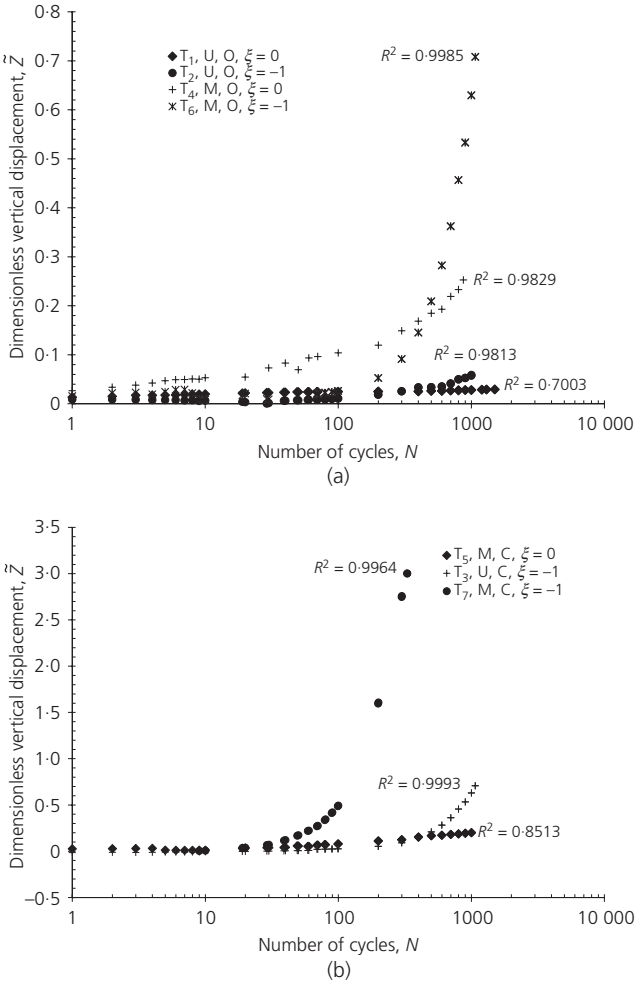

Figure 10. (a) Vertical upward displacement of open-ended piles for uni-directional and multi-directional (one-way and two-way) loading. (b) Vertical upward displacement of closed-ended piles for uni-directional and multi-directional (one-way and two-way) loading

5.4 Comparison between open- and closed-ended piles

Under multi-directional one-way loading ($\xi = 0$) the closed-ended pile had 18% higher stiffness than the open-ended pile at $N = 1000$ (Figure 7(b)). The closed-ended pile had about half the lateral displacement of the open-ended pile (Figure 8(a)). This indicates that the base shear resistance has a significant role in resisting the horizontal load for closed-ended rigid piles. The lower displacement and higher stiffness indicate a higher rate of passive resistance developed along the pile's length for closed-ended piles in comparison with the open-ended piles. Since the only difference between the open- and closed-ended piles studied in this investigation is the pile base condition, it may be concluded that the closed-ended condition (achieved by using a steel base) generates faster passive resistance along the pile's length.

Under two-way uni-directional loading ($\xi = -1$) the closed-ended pile had 30% lower stiffness compared to the open-ended pile at $N = 1000$ (Figure 7(a)). No significant difference in horizontal displacement was observed between the closed-ended and open-ended piles (Figure 8(b)). The closed-ended pile had much higher vertical upward movements compared to the open-ended pile (Figures 10(a) and 10(b)). This may be due to the additional uplift force created at the base of the pile

Downloaded by [TU Delft Library] on [08/02/17]. Copyright © ICE Publishing, all rights reserved.

from the flow of sand below the base as the pile rotates. This observation on vertical upward movement needs further field verification on large-diameter concrete piles under cyclic loading.

5.5 Comparison between uni-directional and multi-directional loading

The present investigation suggests significant differences in the pile response between uni-directional and multi-directional cyclic loading. Under one-way cyclic loading ($\xi = 0$) the piles under multi-directional loading had a 28% higher stiffness than the piles subjected to uni-directional loading (Figure 7(b)). For $\xi = 0$, multi-directional loading produced about six times higher radial displacement (u_N/u_1) (Figure 8(a)) and nine times higher vertical displacement ($\tilde{Z}$) (Figure 10(a)) in comparison to the uni-directional loading. The high accumulated displacement in the multi-directional loading may be due to the involvement of a much higher volume of soil mass in the shearing process compared to that of the uni-directional loading. Under $\xi = 0$ and multi-directional loading, half of the soil mass adjacent to the pile experienced periodic passive conditions and the other half of the soil mass experienced periodic active conditions. This led to two different kinds of soil structure on each side of the pile, increasing the stiffness compared to uni-directional loading. The present experimental investigation suggests that this type of change in soil structure due to multi-lateral loading increases the stiffness of the soil–pile system compared to that of uni-directional loading.

Under two-way cyclic loading ($\xi = -1$), the piles that were subjected to multi-directional loading had a lower stiffness when compared to those subjected to uni-directional loading (Figure 7(c)). In the case of $\xi = -1$, the multi-directional loading causes the adjacent soil mass to experience periodic passive and active conditions on both sides of the pile. As a result, the soil structure continuously forms and is then destroyed, resulting in higher numbers of load cycles to develop a stable sand structure. The multi-directional load also yielded three to five times higher vertical displacement and three times the radial displacement.

6. Conclusions

The research reported in this paper investigated the performance of monopiles under uni-directional and multi-directional lateral cyclic loading. Two types of cyclic loading defined as two-way ($\xi = -1$) and one-way ($\xi = 0$) have been used for the investigation. Tests were carried out on a model monopile 530 mm long and 90 mm in diameter, embedded into a sand bed of initial relative density of 77%. Effects of pile end conditions (open- and closed-ended) were also investigated.

The dimensionless stiffness of the soil–pile system under cyclic horizontal loading increased with the number of load cycles (N). Multi-directional one-way ($\xi = 0$) cyclic loading produced significantly higher stiffness compared to the piles subjected to uni-directional cyclic loading under the same number of load cycles and pile conditions. Multi-directional $\xi = 0$ cyclic loading produced much higher horizontal displacements than uni-directional cyclic loading. Significant vertical deformation was observed under multi-directional $\xi = 0$ cyclic loading. An open-ended pile developed more horizontal displacement than a similar closed-ended pile. The stiffness did not increase significantly under multi-directional two-way ($\xi = -1$) cyclic loading. Multi-directional as well as uni-directional two-way ($\xi = -1$) cyclic loading produced less horizontal displacement than one-way ($\xi = 0$) cyclic loading. Higher vertical displacement was observed under two-way ($\xi = -1$) multi-directional cyclic loading in comparison to one-way ($\xi = 0$) multi-directional cyclic loading. The observed stiffness and displacement can be expressed mathematically by logarithmic and power functions, respectively.

REFERENCES

Achmus M, Kuo YS and Rahman KD (2009) Behavior of monopile foundations under cyclic lateral load. *Computers and Geotechnics* **36(5)**: 725–735.

Alizadeh M and Davisson MT (1970) Lateral load test on piles-Arkansas river project. *Journal of the Soil Mechanics and Foundations Division, ASCE* **96(5)**: 1583–1604.

API (American Petroleum Institute) (2000) *RP 2A-WSD: Recommended Practice for Planning, Designing and Constructing Fixed Offshore Platforms–Working Stress Design*, 21st edn. American Petroleum Institute, Washington, DC, USA.

Arshad M and O'Kelly BC (2016) Piled-cruciform attachment to monopile head reduces deflection. *Proceedings of the Institution of Civil Engineers – Geotechnical Engineering* **169(4)**: 321–335, http://dx.doi.org/10.1680/jgeen.15.00001.

Bhattacharya S, Nikitas N, Garnsey J *et al.* (2013) Observed dynamic soil–structure interaction in scale testing of offshore wind turbine foundations. *Soil Dynamics and Earthquake Engineering* **54**: 47–60.

Bienen B, Duhrkop J, Grabe J, Randolph MF and White DJ (2012) Response of piles with wings to monotonic and cyclic lateral loading in sand. *Journal of Geotechnical and Geoenvironmental Engineering* **138(3)**: 364–375.

Chen RP, Sun YX, Zhu B and Gou WD (2015) Lateral cyclic pile–soil interaction studies on a rigid model monopile. *Proceedings of the Institution of Civil Engineers – Geotechnical Engineering* **168(2)**: 120–130, http://dx.doi.org/10.1680/geng.14.00028.

Cui L and Bhattacharya S (2016) Soil–monopile interactions for offshore wind turbines. *Engineering and Computational Mechanics* **169(4)**: 171–182, http://dx.doi.org/10.1680/jencm.16.00006.

DNV (Det Norske Veritas) (2011) DNV-OS-J101: Design of offshore wind turbine structures. DNV, Veritasveien, Norway.

Dyson GJ and Randolph MF (2001) Monotonic lateral loading of piles in calcareous sand. *Journal of Geotechnical and Geoenvironmental Engineering* **127(4)**: 346–352.

Houlsby GT, Ibsen LB and Byrne W (2005) Suction caissons for turbines. In *Frontiers in Offshore Geotechnics, ISFOG 2005* (Gourvenec S and Cassidy M (eds)). Taylor & Francis Group, London, UK, pp. 75–93.

Leblanc C, Houlsby GT and Byrne BW (2010) Response of stiff piles in sand long-term cyclic lateral loading. *Géotechnique* **60(2)**: 79–90.

Lesny K and Hinz P (2009) Design of monopile foundations for offshore wind energy converters. In *Contemporary Topics in Deep Foundations* (Iskander M, Laefer DF and Hussein MH (eds)).

Downloaded by [TU Delft Library] on [08/02/17]. Copyright © ICE Publishing, all rights reserved.

American Society of Civil Engineers (ASCE), Reston, VA, USA, pp. 512–519.

Li Z, Haigh SK and Bolton MD (2010) Centrifuge modelling of mono-pile under cyclic lateral loads. *Proceedings of 7th International Conference on Physical Modelling in Geotechnics, Zurich, Switzerland*, vol. 2, pp. 965–970.

Li W, Igoe D and Gavin K (2015) Field tests to investigate the cyclic response of monopiles in sand. *Proceedings of the Institution of Civil Engineers – Geotechnical Engineering* **168(5)**: 407–421, http://dx.doi.org/10.1680/jgeen.14.00104.

Little RL and Briaud JL (1988) *Full Scale Cyclic Lateral Load Tests on Six Single Piles in Sand*. Geotechnical Division, Civil Engineering Department, Texas A&M University, College Station, TX, USA, paper GL-88-27.

Murchison JM and O'Neill MW (1984) Evaluation of *p–y* relationships in cohesionless soils. In *Analysis and Design of Pile Foundations* (Meyer JR (ed.)). American Society of Civil Engineers (ASCE), New York, NY, USA, pp. 174–191.

Murphy G, Doherty P, Cadogan D and Gavin K (2016) Field experiments on instrumented winged monopiles. *Proceedings of the Institution of Civil Engineers – Geotechnical Engineering* **169(3)**: 227–239, http://dx.doi.org/10.1680/jgeen.15.00134.

Peng J, Clarke BG and Rouainia M (2011) Increasing the resistance of piles subjected to cyclic lateral loading. *Journal of Geotechnical and Geoenvironmental Engineering* **137(10)**: 977–982.

Reese LC and Van Impe WF (2011) *Single Piles and Pile Groups Under Lateral Loading*. CRC Press, Taylor and Francis, London, UK.

Rudolph C, Bienen B and Grabe J (2014) Effect of variation of the loading direction on the displacement accumulation of large piles under cyclic lateral loading in sand. *Canadian Geotechnical Journal* **51(10)**: 1196–1206.

Sathialingam N and Kutter BL (1989) *The Effects of High Strain Rate and High Frequency Loading on Soil Behavior in Centrifuge Model Tests*. Naval Civil Engineering Laboratory, Port Hueneme, CA, USA.

Schneider J and Senders M (2010) Foundation design – a comparison of oil and gas platforms with offshore wind turbines. *Journal of the Marine Technology Society* **44(1)**: 32–51.

Seidel M (2010) Feasibility of monopiles for large offshore wind turbines. *Proceedings of the 10th German Wind Energy Conference (DEWEK 2010), Bremen, Germany*, pp. 1–4.

Tucker LM and Briaud JL (1988) *Analysis of the Pile Load Test Program at Lock and Dam 26 Replacement Project*. Geotechnical Division, Civil Engineering Department, Texas A&M University, College Station, TX, USA, paper GL-88-11.

How can you contribute?

To discuss this paper, please email up to 500 words to the editor at journals@ice.org.uk. Your contribution will be forwarded to the author(s) for a reply and, if considered appropriate by the editorial board, it will be published as discussion in a future issue of the journal.

Proceedings journals rely entirely on contributions from the civil engineering profession (and allied disciplines). Information about how to submit your paper online is available at www.icevirtuallibrary.com/page/authors, where you will also find detailed author guidelines.

Downloaded by [TU Delft Library] on [08/02/17]. Copyright © ICE Publishing, all rights reserved.